Multiband wavelength-division demultiplexing with a cascaded substrate-mode grating structure

Yi-Kong Tsai, Yang-Tung Huang, and Der-Chin Su

A multiband wavelength-division-demultiplexing (WDDM) structure, which incorporates cascaded substrate-mode holograms, is presented. The method can be used to design a WDDM device that consists of two or more layers of fundamental units (i.e., substrate-mode holograms). The fundamental unit is based on a diffracted grating and a substrate that include angular dispersion, wavelength bandwidth, and total internal reflection, which can be used to separate optical signals of different wavelengths. We have designed and built a multiband WDDM device, incorporating cascaded substrate-mode holograms in dichromated gelatin.

Key words: Wavelength-division demultiplexing, substrate-mode hologram.

1. Introduction

Wavelength-division multiplexing (WDM) has been identified as an important technique that can be used to increase the information-carrying capacity of a single-fiber communication link.[1–3] A holographic element is an angularly dispersive device that can be used to separate optical signals of different wavelengths.[4,5] This angularly dispersive device has the advantage of compactness for dense wavelength-division-demultiplexing (WDDM) applications to a large number of channels. For such applications, passband width and polarization-insensitive high efficiency must be considered.

The transmission-type and reflection-type substrate-mode holographic grating pairs have been investigated for WDDM applications.[6,7] However, the number of channels for this device is still limited. In this paper we present a cascaded substrate-mode hologram structure that can be used to increase the operation of channel numbers. WDDM devices of cascaded substrate-mode holographic structures are compact and can significantly increase the capacity of demultiplexing channel numbers. The fundamental unit of the cascade structure is composed of a grating pair and a substrate, formed as a substrate-mode holographic structure. This type of substrate-mode hologram diffracts normally incident beams into a dielectric substrate with total internal reflection. The diffracted beams then propagate through the substrate and are coupled out with on-axis imaging. Normally incident coupling and on-axis imaging with this structure provide easier alignment with optical fibers. A three-layer device with an insertion loss of less than 2.0 dB has been fabricated, which can be used for 60-channel operation with 2-nm channel spacing and 125-μm output fiber separation. In our discussions the insertion loss means the loss that is due to signal propagation through our holographic WDDM devices.

2. Wavelength-Division Demultiplexing of Cascaded Substrate-Mode Holographic Configurations

WDM systems could significantly increase the transmission capacity of existing optical fiber systems. We report a cascaded structure of substrate-mode holographic grating pairs for WDDM applications in multiband dense WDM systems. Figure 1 shows the configuration of a two-layer substrate-mode holographic grating pair. Based on the diffraction properties of holographic gratings for specific center wavelengths of 780, 1050, 1300, and 1550 nm, the WDDM device of a cascaded structure can be fabricated. As a demultiplexer, combined beams of several wavelength bands, λ_{11}, λ_{12}, λ_{13}, . . . and λ_{21}, λ_{22}, λ_{23}, . . . , enter the device from fiber that is collimated by a graded-index (GRIN) rod lens. The collimated beams strike the holographic grating (H_{I1}) of the 1st layer and are separated into two group wavelengths (λ_{1n}

The authors are with the National Chiao Tung University, 1001 Ta-Hsueh Road, Hsin-Chu, Taiwan. Y-K. Tsai and D-C. Su are in the Institute of Electro-Optical Engineering, Y-T. Huang is in the Department of Electronics Engineering and Institute of Electronics.

Received 26 July 1994; revised manuscript received 10 March 1995.

0003-6935/95/255582-07$06.00/0.

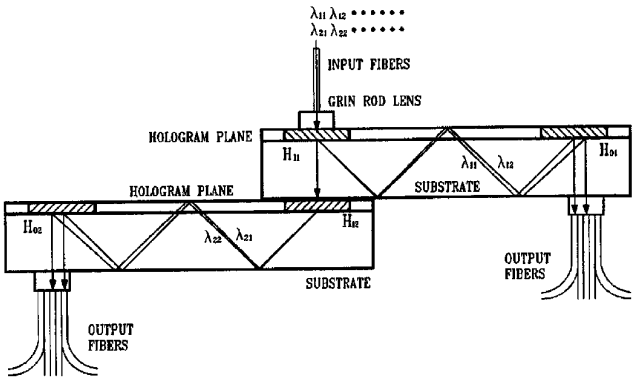

Fig. 1. Cascaded connection configuration of two-layer substrate-mode holograms for a WDDM.

and λ_{2n}) according to the angular dispersion and diffraction property. The diffracted beams (λ_{1n}) that propagate through the 1st substrate and grating H_{O1} are separated and coupled into the 1st bundle of output fibers. The directly transmitted beams (λ_{2n}) from grating H_{I1} that enter grating H_{I2} diffract, propagate through the 2nd substrate and grating H_{O2}, and separate into a 2nd bundle of output fibers. For such a cascaded structure, it would obviously be desirable to be able to increase the capacity of the system without a significant design change and more complex fabrication.

To design the demultiplexers of a cascaded structure there are four characteristic parameters that must be considered: (1) insertion loss of each fundamental unit, (2) cross-talk attenuation between channels in each fundamental unit, (3) cross-talk attenuation between elements, and (4) polarization characteristics of each grating.

We use a transmission-type substrate-mode holographic grating pair as the fundamental unit of a cascaded optical demultiplexing device. According to coupled-wave theory,[8] the diffraction efficiencies of *s*- and *p*-polarization fields for a transmission phase grating with medium thickness *d* are given by

$$\eta = \frac{\sin^2(\nu^2 + \xi^2)^{1/2}}{1 + \xi^2/\nu^2}, \tag{1}$$

where

$$\nu = \nu_s = \frac{\pi n_1 d}{\lambda_r(\cos\theta_{r1}\cos\theta_{r2})^{1/2}} \text{ for } s \text{ polarization}, \tag{2a}$$

$$\nu = \nu_p = \nu_s \cos(\theta_{r2} - \theta_{r1}) \text{ for } p \text{ polarization}, \tag{2b}$$

$$\xi = \frac{\vartheta d}{2\cos\theta_{r2}}, \tag{3}$$

λ_r is the reconstruction wavelength, *d* is the hologram emulsion thickness, n_1 is the amplitude of the refractive-index modulation, ϑ is the dephasing factor, and θ_{r1} and θ_{r2} are the corresponding angles of the reconstruction and diffracted beams in the hologram emulsion, respectively. When the reconstruction is at the Bragg condition, i.e., $\xi = 0$, the diffraction efficiency of this grating is maximum; when it is at the off-Bragg condition, the efficiency is reduced.

The diffraction efficiency depends on the hologram thickness, the grating-index modulation, the diffraction angle, and the angular deviation from the Bragg angle. In our devices, the index modulation n_1 is 0.023, 0.030, 0.037, and 0.045 for center wavelengths of 780, 1050, 1300, and 1550 nm, respectively, and the corresponding diffraction efficiencies for the *s*- and *p*-polarization fields as functions of reconstruction center wavelengths of 780, 1050, 1300, and 1500 nm are shown in Figs. 2(a)–2(d), respectively. These figures show that the desired polarization-insensitive characteristics and the bandwidths of the less than 0.7-dB insertion loss for both *s*- and *p*-polarization fields are 30, 39, 52, and 72 nm for center wavelengths of 780, 1050, 1010, and 1550 nm, respectively. A longer wavelength gives a broader bandwidth. Using these results, we investigated various structures for multiband WDDM.

3. Design of the Two-Layer Configuration

A. Two-Layer Configuration for Center Wavelengths of 780 and 1300 nm

In order to increase the number of WDDM channels, we propose a cascaded connection structure. From Figs. 2(a) and 2(c) we can design a multiband WDDM device with two layers of substrate-mode holographic grating pairs that can be used to separate 780- and 1300-nm group wavelength beams. The 1st layer with reconstruction angle $\theta_{r1}^{780} = 0°$ and diffracted angle $\theta_{r2}^{780} = 45°$ was designed for a center wavelength of 780 nm, the 2nd layer with $\theta_{r1}^{1300} = 0°$ and $\theta_{r2}^{1300} = 45°$ was designed for a center wavelength of 1300 nm. H_{I1}^{780} diffracts the incident beams of the 780-nm group wavelengths at an angle that exceeds the critical angle of the substrate that supports the recording material and directly transmits the beams of the 1300-nm group wavelengths and the diffracted residual of the 780-nm group wavelengths. The corresponding wavelength sensitivities of diffraction efficiencies are shown in Fig. 2(a), from which it can be seen that the efficiencies are $\eta_s = 96\%$ and $\eta_p = 95\%$ for 780 nm and the efficiencies are $\eta_s \simeq \eta_p \simeq 0$ for 1300 nm. The diffracted beams then propagate through the substrate with multiple total internal reflections to the output coupling grating H_{O1}^{780} and are normally coupled out to the corresponding optical fibers for specific wavelengths. The grating H_{I2}^{1300} diffracts the transmitted beams from H_{I1}^{780} at angles of 11.2° and 45° for wavelengths of 780 and 1300 nm, respectively, and the corresponding efficiencies are shown in Fig. 2(c). In the same way, the diffracted beams of 1300-nm group wavelengths propagate through the substrate with multiple total internal reflections to the output grating H_{O2}^{1300} and are coupled out to optical fibers.

For a cascaded structure, the passband width of the diffracted efficiency higher than 85% (−0.7 dB) was approximately 30 and 35 nm for a center wavelength

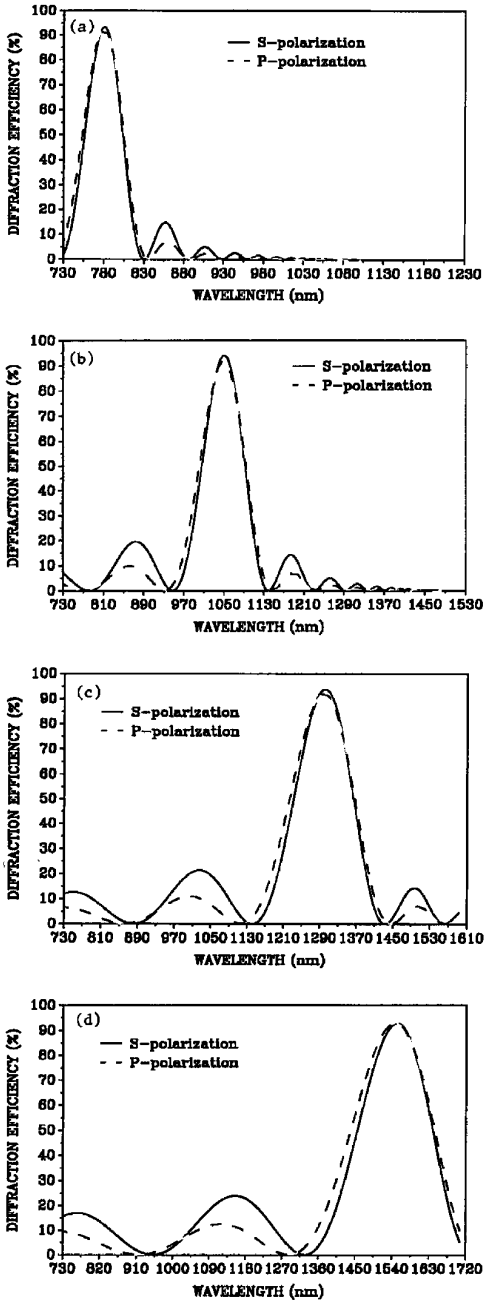

Fig. 2. Calculated *s*- and *p*-polarization diffraction efficiencies of substrate-mode gratings for center wavelengths of (a) 780, (b) 1050, (c) 1300, (d) 1550 nm.

of 780 and 1300 nm, respectively. Using a typical 125-μm separation for an output fiber array, the required lateral distance between input and output gratings is 2.6 cm with 2-nm channel spacing. In this structure the total number of demultiplexed channels is 32 and the insertion loss is less than 1.4 dB.

B. Two-Layer Configuration for Center Wavelengths of 1300 and 1550 nm

Similar devices that operate at 1300- and 1550-nm group wavelengths can also be designed with the same method as discussed in Subsection 3.A. In this structure the efficiencies of the 1st and 2nd layers are shown schematically in Figs. 2(c) and 2(d), respectively. The device can be used to separate optical wavelength regions between 1274–1326 and 1528–1584 nm with an insertion loss of less than 1.4 dB, as shown in Fig. 3, and cross-talk levels from other wavelength bands compared with the signal at a center wavelength of less than −30 dB. Figure 3 shows the output diffraction efficiencies of the 1300- and 1550-nm center wavelengths when the light propagates through the two layers. With 2-nm channel spacing, 56 channels can be demultiplexed in this two-layer structure.

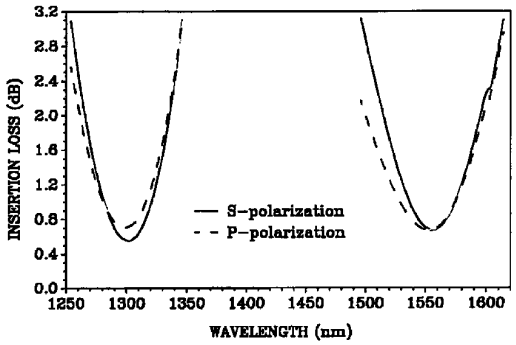

Fig. 3. Theoretical output efficiencies of incident light when it propagates through a two-layer structure for center wavelengths of 1300 and 1550 nm.

4. Design of the Four-Layer Configuration

Figure 4 shows the four-layer configuration, for which the passband characteristics of each layer are shown in Fig. 2. The center wavelength of layer 1 is 780 nm; that is, a light beam of a near-center wavelength of 780 nm is diffracted by grating H_{I1}. However, the group wavelengths of 1050, 1300, and 1550 nm are sufficiently different from 780 nm and are transmitted by layer 1. Similarly, the center wavelengths of high diffraction efficiencies for layers

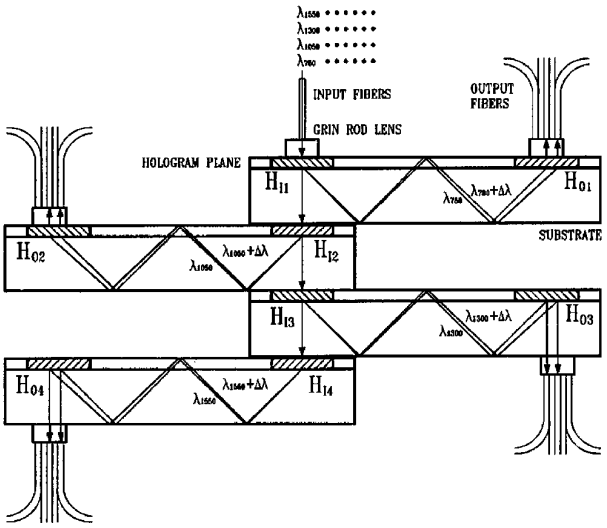

Fig. 4. Cascaded structure of four-layer transmission-type grating pairs at center wavelengths of 780, 1050, 1300, and 1550 nm.

2–4 are 1050, 1300, and 1550 nm, respectively, and each layer transmits wavelengths that are sufficiently different from its specific center wavelength. The collimated light signals in these four wavelength bands enter layer 1. Because of the diffraction characteristics of layer 1, the light near the 780-nm wavelength is diffracted into the substrate of layer 1, whereas others are directly transmitted and enter layer 2. The group beams of 780 nm are angularly dispersed, according to different wavelengths, and diffracted at higher than the critical angle within the substrate. Then these beams pass through the substrate, are diffracted by grating H_{O1}, and are coupled out to their corresponding output fibers. In the same way, the beams of group wavelengths 1050, 1300, and 1550 nm are separated in sequence through layers 2, 3, and 4, respectively. In this device a combination of a substrate-mode holographic grating pair is employed to obtain a large number of demultiplexed channels. The simulation results of spectral response for the insertion loss caused by signal propagation through the holographic WDDM device are shown in Fig. 5. Consider the WDDM design with an insertion loss of less than 1.4 dB and interchannel wavelength spacing of 2 nm. The device can operate for approximately 87 channels, including 15, 18, 25, and 29 channels for four layers of center wavelengths of 780, 1050, 1300, and 1550 nm, respectively. The cascaded four-layer configuration is attractive because it is compact, provides high capacity, and offers the possibility of relatively inexpensive production processes.

5. Experimental Results

An improvement in WDM characteristics using a cascaded substrate-mode holographic structure, including an increase in the number of demultiplexed channels in a given spectral region, minimization of optical losses, and cross talk, is strongly dependent on angular bandwidth, wavelength bandwidth, and cross-talk attenuation of each fundamental unit, which is composed of a grating pair and substrate. In our experiments these fundamental units are volume-transmission substrate-mode holograms formed in dichromated gelatin (DCG) and exhibit characteristics of high diffraction efficiency, low scattering noise, and negligible absorption. Each fundamental unit for a specific center wavelength was fabricated separately. Our DCG material was prepared by use of a Kodak 649F photographic plate and the simplified procedure presented by Georgekutty and Liu.[9] For convenience of fabrication and performance requirements of optical fiber communications, to fabricate each grating we used the shorter wavelength free-space recording at 488-nm wavelength and designed the readout wavelength for the infrared region.[10] The use of DCG demonstrates the concept of a cascaded structure, with the reconstruction beam illuminating the grating at normal incidence, the recording material with an average refractive index of 1.54 and thickness of 17 μm, and a dielectric substrate with a 1.523 refractive index for the 488-nm wavelength. The center wavelength beam diffracts at 45° to the normal within the emulsion.

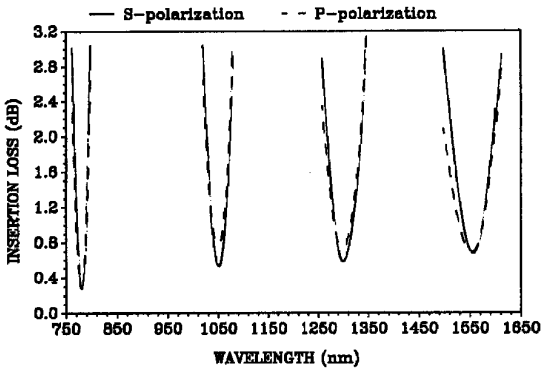

Fig. 5. Spectral response of a four-layer structure at the output ends.

The schematic diagram of the cascaded structure setup for implementation of WDDM is shown in Fig. 1. In our experiments device characteristics for three examples of cascaded structures with no fiber coupling were measured. First, three fundamental units of substrate-mode holograms for center wavelengths of 780, 1300, and 1550 nm were fabricated separately. Second, at reconstruction we measured the wavelength bandwidth of these fundamental units that can be used to determine the number of demultiplexed channels. Figure 6 shows the experimental data for diffraction efficiencies of substrate-mode gratings as a function of wavelength for center wavelengths of 780, 1300, and 1550 nm. The near-center wavelength ranges were obtained directly from our diode laser system, whereas other data were extracted from the angular response as shown in Fig. 7. From the measured data of Fig. 7, the wavelength bandwidth can be calculated from Eqs. (1)–(3).

To evaluate the potential and limitations of the cascaded substrate-mode structure, the results of three examples were carried out.

A. Two-Layer Configuration for Center Wavelengths of 780 and 1300 nm

The WDDM structure of the two-layer design illustrated in Fig. 1 uses a demultiplexer to separate the signals of different wavelengths. The center wavelengths for the 1st and 2nd layers are 780 and 1300 nm, respectively. The experimental wavelength sensitivities of diffraction efficiencies for *s* and *p* polarizations are shown in Figs. 6(a) and 6(b). In the measurements, it can be seen that the diffraction efficiency of input grating $H_{I1}{}^{780}$ of the 1st layer is $\eta_s \simeq \eta_p \simeq 0$ for 1300 nm. We have now constructed and tested a two-band WDDM of a substrate-mode structure. The insertion losses of the two-layer configuration that are due to the beam propagation through these holographic WDDM devices were measured as shown in Fig. 8. The interchannel wavelength spacing of each layer was 2 nm, the insertion losses were less than 2.0 dB, the cross talk from other wavelength

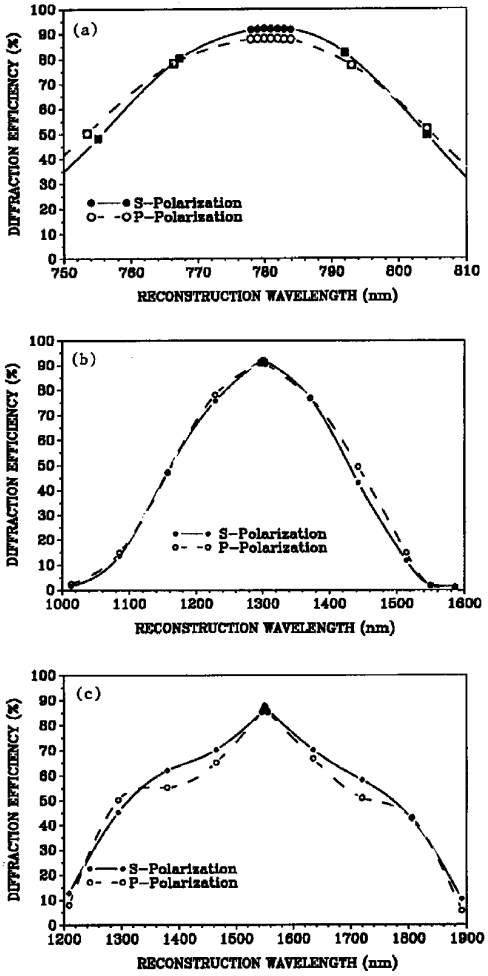

Fig. 6. Experimental diffraction efficiencies of the WDDM device for center wavelengths of (a) 780, (b) 1300, and (c) 1550 nm. The near-center wavelength ranges were obtained directly from our diode laser system, whereas other data were extracted from the angular response as shown in Fig. 7.

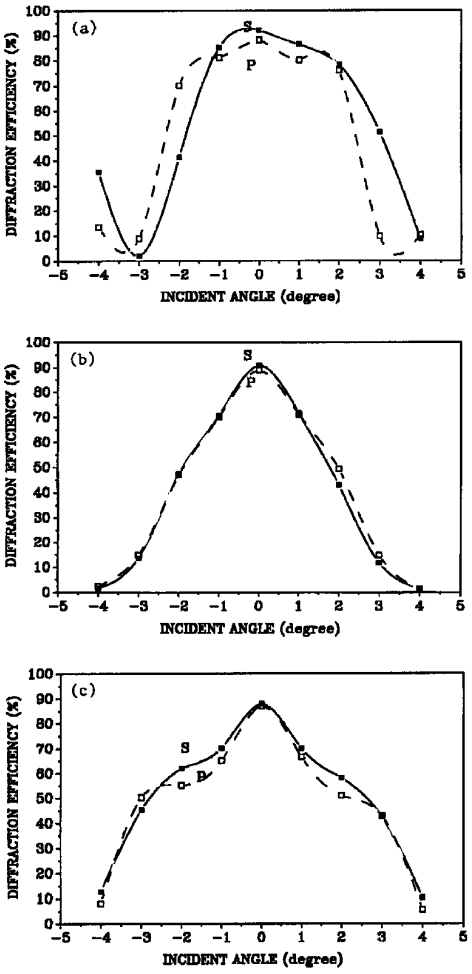

Fig. 7. Measured angular bandwidth of the fundamental units for center wavelengths of (a) 780, (b) 1300, and (c) 1550 nm.

bands compared with the signal at the center wavelength was < -20 dB, and the total number of channels is expected to be 36.

B. Two-Layer Configuration for Center Wavelengths of 1300 and 1550 nm

In a similar situation as that outlined in Subsection 5.A, the experimental data of Figs. 6(b) and 6(c) indicate that the diffraction efficiencies of $H_{I1}{}^{1300}$ are $\eta_s = 2.1\%$ and $\eta_p = 1.8\%$ for the 1550-nm center wavelength of the 2nd layer. Therefore, the diffracted property of input grating $H_{I1}{}^{1300}$ will induce the reduction of the output efficiencies of the 2nd layer. Here we obtained the experimental data in Fig. 9 for a cascaded structure with which we intend to achieve the expected total channel number of 47 with an interchannel wavelength spacing of 2 nm, an insertion loss of <2.0 dB, and cross talk from other wavelength bands compared with the less than -20-dB signal at the center wavelength.

C. Three-Layer Configuration for Center Wavelengths of 780, 1300, and 1550 nm

Based on the analytic data in Fig. 6, the optimum setup of the cascaded structure is arranged in center wavelengths of 780, 1300, and 1550 nm for the 1st, 2nd, and 3rd layers. This arrangement can be used to achieve the maximum transmission channels. Using 1550 nm as the reconstruction source yields

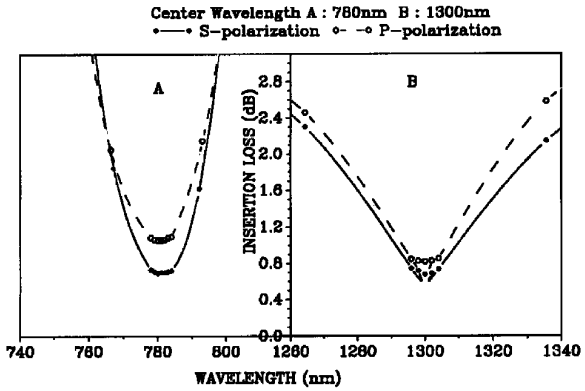

Fig. 8. Experimental spectral response of a two-layer structure for center wavelengths of 780 and 1300 nm.

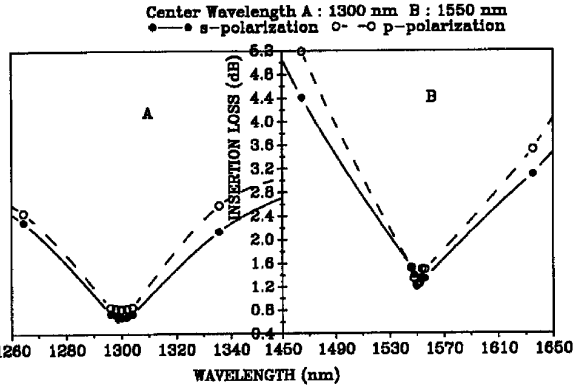

Fig. 9. Experimental spectral response of a two-layer structure for center wavelengths of 1300 and 1550 nm.

diffraction efficiencies of $\eta_s^{1st} \simeq \eta_p^{1st} \simeq 0$, $\eta_s^{2nd} = 2.1\%$, $\eta_p^{2nd} = 1.8\%$, $\eta_s^{3rd} = 88\%$, and $\eta_p^{3rd} = 87\%$ for input gratings H_{I1}^{780}, H_{I1}^{1300}, and H_{I1}^{1550} of the 1st to 3rd layers. For the reconstruction wavelength of 1300 nm, the diffraction efficiencies are $\eta_s^{1st} \simeq \eta_p^{1st} \simeq 0$, $\eta_s^{2nd} = 92.2\%$, and $\eta_p^{2nd} = 90.6\%$. Figure 10 shows experimental data of insertion loss versus three passband wavelengths for the three-layer cascaded structure. The three-layer device has wavelength bandwidths of 26, 46, and 48 with an insertion loss of less than 2.0 dB for the 1st to 3rd layers, respectively. The corresponding channels of 1st to 3rd layers are expected to be 13, 23, and 24 with an interchannel wavelength spacing of 2 nm.

The experimental results show the capacity of a three-layer structure to achieve a total demultiplexed channel number of 60, an insertion loss of <2.0 dB, and cross talk from other wavelength bands compared with the signal at the center wavelength of < -20 dB. These results strongly suggest that a cascaded substrate-mode structure could be used to make a compact WDDM device, separate multiband signals, and enhance demultiplexing capacity.

In our experiments we have not included the characteristic degradation that is due to fiber coupling inaccuracy. However, normal coupling with these holographic devices can provide better alignment accuracy compared with other holographic

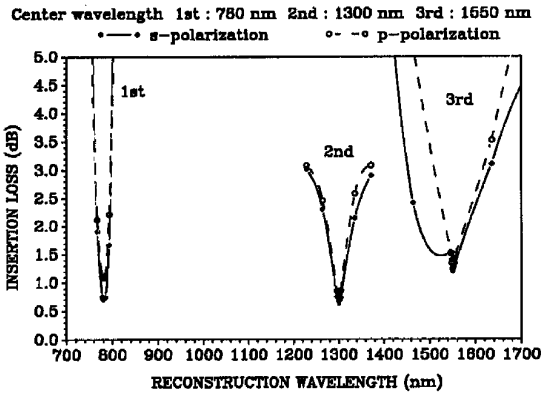

Fig. 10. Experimental performance efficiencies of a three-layer structure for center wavelengths of 780, 1300, and 1550 nm.

WDDM devices.[5] The misalignment that is due to wavelength shifts of semiconductor laser sources has not been discussed. To realize the applications of all WDDM devices, these wavelength-shift characteristics need to be investigated further.

6. Summary and Discussions

We have described cascaded connection-type substrate-mode holographic gratings for the application of multiband wavelength-division demultiplexing. The multichannel dense WDDM structure was designed and evaluated. Many different embodiments of the device are possible, based on the use of many different types of substrate-mode holographic grating pair combination. Each single-layer element that is capable of isolating one group of wavelengths from others has been experimentally constructed. We obtained key characteristics of a substrate-mode holographic structure that directly affects the optimum cascaded structure design, such as wavelength sensitivity and angular dispersion. These factors helped us to determine the overall design of the cascaded prototypes that we fabricated. With the cascaded transmission-type holographic structure that consists of three layers, a separation of three group wavelengths and a 2-nm refinement between adjacent signals were implemented. By using the three-layer structure, we achieved a less than 2.0-dB insertion loss as a result of beam propagation through the holographic WDDM device, and 60 demultiplexing channels are expected. With the low insertion losses, multiplexer–demultiplexers with a large number of channels can be contemplated, and simultaneous operation in two directions should be feasible.

The research was supported by the National Science Council of the Republic of China under contract NSC83-0417-E009-030. The reviewers' helpful suggestions are greatly appreciated.

References

1. H. Ishio, J. Minowa, and K. Nosu, "Review and status of wavelength-division-multiplexing technology and its applications," IEEE J. Lightwave Technol. **LT-2,** 448–463 (1984).
2. L. Jou, and B. Metcalf, "Wavelength division multiplexing," in *Future Trends in Fiber Optic Communication,* C. W. Kleekamp, ed., Proc. Soc. Photo-Opt. Instrum. Eng. **340,** 69–74 (1982).
3. J. Lipson, W. J. Minford, E. J. Murphy, T. C. Rice, R. A. Linke, and G. T. Harvey, "A six-channel wavelength multiplexer and demultiplexer for single mode systems," IEEE J. Lightwave Technol. **LT-3,** 1159–1163 (1985).
4. M. Lida, H. Asakura, K. Eda, and K. Hagiwara, "Narrow-band ten-channel optical multiplexer and demultiplexer using a Fourier diffraction grating," Appl. Opt. **31,** 4015–4057 (1992).
5. B. Moslehi, P. Harvey, J. Ng, and T. Jannson, "Fiber-optic wavelength-division multiplexing and demultiplexing using volume holographic gratings," Opt. Lett. **14,** 1088–1090 (1989).
6. Y.-T. Huang, D.-C. Su, and Y.-K. Tsai, "Wavelength-division-multiplexing and demultiplexing by using a substrate-mode grating pair," Opt. Lett. **17,** 1629–1631 (1992).
7. Y.-K. Tsai, Y.-T. Huang, and D.-C. Su, "A reflection-type substrate-mode grating structure for wavelength-division-multi/demultiplexing," Optik **97,** 62–66 (1994).

8. H. Kogelnik, "Coupled wave theory for thick hologram gratings," Bell Syst. Tech. J. **48,** 2909–2947 (1969).
9. T. G. Georgekutty and H.-K. Liu, "Simplified dichromated gelatin hologram recording process," Appl. Opt. **26,** 372–376 (1987).
10. Y.-T. Huang, M. Kato, and R. K. Kostuk, "Methods for fabricating substrate-mode holographic optical elements," in *Computer and Optically Formed Holographic Optics*, I. Cindrich and S. H. Lee, eds., Proc. Soc. Photo-Opt. Instrum. Eng. **1211,** 162–172 (1990).